Influence of the Shape of Power Supply Waveform on Power Quality and Optical Parameters of Selected Light Sources

Przemysław Ptak *, Tadeusz Lorkowski, Krzysztof Górecki

Posted Date: 17 March 2026

doi: 10.20944/preprints202603.1372.v1

Keywords: fluorescent lamp; LED lamp; solid-state light sources; power supply waveform; power factor correction; power quality; power analysis; total harmonic distortion

 doi:10.20944/preprints202603.1372.v1

Article

Influence of the Shape of Power Supply Waveform on Power Quality and Optical Parameters of Selected Light Sources

Przemysław Ptak [1,*], Tadeusz Lorkowski [2] and Krzysztof Górecki [1]

[1] Department of Power Electronics, Faculty of Electrical Engineering, Gdynia Maritime University, Morska 81-87, 81-225 Gdynia, Poland

[2] Faculty of Electrical Engineering, Gdynia Maritime University, Morska 81-87, 81-225 Gdynia, Poland

* Correspondence: p.ptak@we.umg.edu.pl

Abstract

The article describes the results of research on the power supply quality of selected fluorescent lamps and solid-state light sources powered by voltage with different waveforms and supply voltage values. The power factor, total harmonic distortion (THD) factor and values of individual harmonics were measured and their compliance with international standards was assessed. The measurement set-up used and the measurement results obtained with it are described. The results of the experimental research showed that the light sources under consideration did not meet the criteria specified in international standards for the THD factor and the values of individual harmonics, regardless of the shape of the supply voltage waveform. However, it was shown that supplying some light sources with a triangular voltage waveform can increase the illuminance value. On the other hand, the use of a rectangular voltage waveform leads to an increase in the power factor and a decrease in reactive power.

Keywords: fluorescent lamp; LED lamp; solid-state light sources; power supply waveform; power factor correction; power quality; power analysis; total harmonic distortion

1. Introduction

One of the main factors shaping human functioning is light. A breakthrough event that facilitated the maintenance of the desired level of lighting was the invention of the light bulb in the 19th century, independently by Joseph Wilson Swan and Thomas Edison [1]. An incandescent light bulb is a lamp containing a filament that heats up when an electric current flows through it. It is hermetically sealed inside a glass bulb filled with a vacuum or an inert gas [2]. Heating the filament leads to the emission of radiation in the visible light range. Over the years, other sources of light powered by electricity have been developed, such as halogen, fluorescent, sodium and mercury lamps [3].

Contemporary lighting solutions most often consist of lamps based on light-emitting diodes (LEDs) [3]. White light-emitting diodes are based on semiconductor structures capable of emitting blue light. The wavelength of the emitted light depends on the energy gap of the semiconductor material used in the construction of the selected power LED [4,5]. Unlike incandescent bulbs, power LEDs are powered by low-voltage direct current, which, in the case of mains power supply, requires the use of an appropriate controller containing a rectifier and a DC-DC converter [6–9].

Power supply circuits for LED lamps contain inductive and capacitive components, which translates into a reactive load, thus leading to distortion of the current waveform, reduction of the power factor and an increase in harmonic distortion [10,11]. Therefore, it is essential to use power factor correction (PFC) circuits and high-efficiency filters, rectifiers and converters. Incandescent

 doi:10.20944/preprints202603.1372.v1

bulbs have a resistive load, which translates into high power factor values without the need for PFC circuits [12].

Due to the presence of a power supply circuit, LED lamps are much more susceptible to distortions in the waveform of the current drawn from the power grid than standard light sources. In [13], the impact of incandescent bulbs, fluorescent lamps and LED lamps on the quality of electricity was compared. The power factor (*PF*) for incandescent bulbs is usually close to one, while for fluorescent and LED lamps it can drop to around 0.62. The total harmonic distortion (THD_I) of the current was also compared. The harmonic distortion factor for incandescent bulbs is usually close to zero, while for fluorescent and LED lamps it can exceed 90%. In [14], the same parameters were determined for other LED lamps. Some of them were characterized by higher power quality, achieving a *PF* above 0.9 and a THD_I below 5%.

Modern light sources should achieve power factor, individual current harmonics (I_k) and THD_I values within the limits specified in technical standards. The requirements for these parameters are specified in IEC 61000-3-2:2018, which also specifies the requirement to use a PFC circuit [15]. The requirements for the total voltage harmonic distortion factor (THD_V) and specific voltage harmonics (V_k) are described in standards IEC 61000-3-3:2013, EN 50160 and IEEE 519-2022 [16–18].

Table 1 presents the permissible values specified in the standard for quantities describing power supply quality, where P denotes power and φ denotes the phase shift between voltage and current.

Table 1. Requirements for power factor and harmonic levels of light sources according to standards IEC 61000-3-2:2018, IEC 61000-3-3:2013 and IEEE 519-2022 [15–18].

Parameter	Light bulb	Fluorescent lamp	LED lamp
PF [15]		does not normalize ($P \le 2$ W)	does not normalize ($P \le 2$ W)
	> 0.5 ($P \le 25$ W)	> 0.4 (2 W < $P \le 5$ W)	> 0.4 (2 W < $P \le 5$ W)
	> 0.9 ($P > 25$ W)	> 0.5 (5 W < $P \le 25$ W)	> 0.5 (5 W < $P \le 25$ W)
		> 0.9 ($P > 25$ W)	> 0.9 ($P > 25$ W)
THD_I [15]	< 23%	< 23%	< 23%
THD_V [16–18]	≤ 8% [16,17]	≤ 8% [16,17]	≤ 8% [16,17]
	≤ 5% [18]	≤ 5% [18]	≤ 5% [18]
I_k [15]	$I_3 < 21.6\%\ I_1$	$I_3 < 21.6\%\ I_1$	$I_3 < 21.6\%\ I_1$
	$I_5 < 10.7\%\ I_1$	$I_5 < 10.7\%\ I_1$	$I_5 < 10.7\%\ I_1$
	$I_7 < 7.2\%\ I_1$	$I_7 < 7.2\%\ I_1$	$I_7 < 7.2\%\ I_1$
	$I_9 < 3.8\%\ I_1$	$I_9 < 3.8\%\ I_1$	$I_9 < 3.8\%\ I_1$
	$I_{11} < 3.1\%\ I_1$	$I_{11} < 3.1\%\ I_1$	$I_{11} < 3.1\%\ I_1$
	$I_{13} < 2.0\%\ I_1$	$I_{13} < 2.0\%\ I_1$	$I_{13} < 2.0\%\ I_1$
	$I_{15} < 0.7\%\ I_1$	$I_{15} < 0.7\%\ I_1$	$I_{15} < 0.7\%\ I_1$
	$I_{17} < 1.2\%\ I_1$	$I_{17} < 1.2\%\ I_1$	$I_{17} < 1.2\%\ I_1$
	$I_{19} < 1.1\%\ I_1$	$I_{19} < 1.1\%\ I_1$	$I_{19} < 1.1\%\ I_1$
	$I_{21} \le 0.6\%\ I_1$	$I_{21} \le 0.6\%\ I_1$	$I_{21} \le 0.6\%\ I_1$
V_k [16]	$V_2 < 2.0\%\ V_1$	$V_2 < 2.0\%\ V_1$	$V_2 < 2.0\%\ V_1$
	$V_3 < 30.0\%\ V_1\cos\varphi$	$V_3 < 30.0\%\ V_1\cos\varphi$	$V_3 < 30.0\%\ V_1\cos\varphi$
	$V_5 < 10.0\%\ V_1$	$V_5 < 10.0\%\ V_1$	$V_5 < 10.0\%\ V_1$
	$V_7 < 7.0\%\ V_1$	$V_7 < 7.0\%\ V_1$	$V_7 < 7.0\%\ V_1$
	$V_9 < 5.0\%\ V_1$	$V_9 < 5.0\%\ V_1$	$V_9 < 5.0\%\ V_1$
	$V_{11}, V_{13}, \ldots, V_{2n+1} < 0.3\%\ V_1$	$V_{11}, V_{13}, \ldots, V_{2n+1} < 0.3\%\ V_1$	$V_{11}, V_{13}, \ldots, V_{2n+1} < 0.3\%\ V_1$

When analyzing the data contained in Table 1, it can be seen that the same permissible values for harmonic distortion and power factor are set for fluorescent lamps and LED lamps. They are mostly the same as for incandescent lamps, with the exception of the power factor, which for rated powers from 2 to 5 W may be lower, and for light sources with even lower powers does not have to

 doi:10.20944/preprints202603.1372.v1

fall within the specified range. For all light sources powered from the mains, $THD_I < 23\%$ and $THD_I < 8\%$ or 5% are permitted, depending on the standard. The requirements for voltage harmonic amplitudes are more stringent than those defined for the current spectrum.

LED lamps are considered to be more environmentally friendly light sources than incandescent or fluorescent lamps [19]. Power electronic circuits and semiconductor structures can also be recycled to obtain raw materials necessary for the electronics industry [20]. Manufacturers of energy-efficient LED lamp controllers can apply for ENERGY STAR® certification. One of the requirements for certified controllers is a power factor $PF \geq 0.5$ for luminaires with a power rating below $P = 5$ W and $PF \geq 0.7$ for luminaires with a power rating above $P = 5$ W [21,22]. Due to the generation of excessive reactive power, a low power factor can lead to inflated electricity bills [23].

The aim of the experimental research was to evaluate the parameters contained in standards [15–18] and to compare these parameters for two LED lamps in relation to a fluorescent lamp, depending on the shape and effective value of the supply voltage. For this purpose, a measuring station was designed and built. Using this stand, the values of selected parameters describing power quality and samples of current and power waveforms were measured and calculated for sinusoidal, square-wave and triangular supply voltages. The results obtained in this way form the basis for assessing the power quality of the light sources under consideration and their compliance with international standards.

The second chapter describes the light sources considered, while the third chapter describes the measuring station used, the measuring method and the mathematical apparatus used. The fourth chapter discusses the results of the experimental research.

2. Tested Light Sources

Experimental tests were conducted on three selected light sources that were adapted to be powered from the mains – a fluorescent lamp and two LED lamps with internal power supply circuits. They were manufactured by different producers. The effective value of the supply voltage for all three lamps is $V_{inRMS} = 230$ V. The basic operating parameters of the light sources under consideration are summarized in Table 2.

Table 2. Operating parameters of the light sources under consideration [24].

Parameter	Compact fluorescent lamp (BRILUX)	LED Lamp 1 (Spectrum)	LED Lamp 2 (LEXMAN)
Maximum luminous flux Φ_V [lm]	1100	1050	1521
Lifetime t_{life} [h]	6000	17000	10000
Rated power P [W]	18	11,5	13,5
Correlated Color Temperature CCT [K]	2700	2700	2700

The light sources under consideration are characterized by a luminous flux ranging from 1100 lm for a fluorescent lamp to 1521 lm for an LED2 lamp (LEXMAN), while the maximum lifetime t_{life} ranges from 6000 h for a fluorescent lamp to 17000 h for an LED1 lamp (Spectrum). The highest rated power P is characteristic of a fluorescent lamp and amounts to 18 W. The correlated color temperature CCT of all tested light sources is the same and amounts to 2700 K.

 doi:10.20944/preprints202603.1372.v1

3. Measurement Set-Up

Figure 1 shows a diagram of the measuring station used to determine the parameters describing the quality of electricity drawn from the power grid and the waveforms of supply voltages and currents, as well as the optical parameters of the tested light sources.

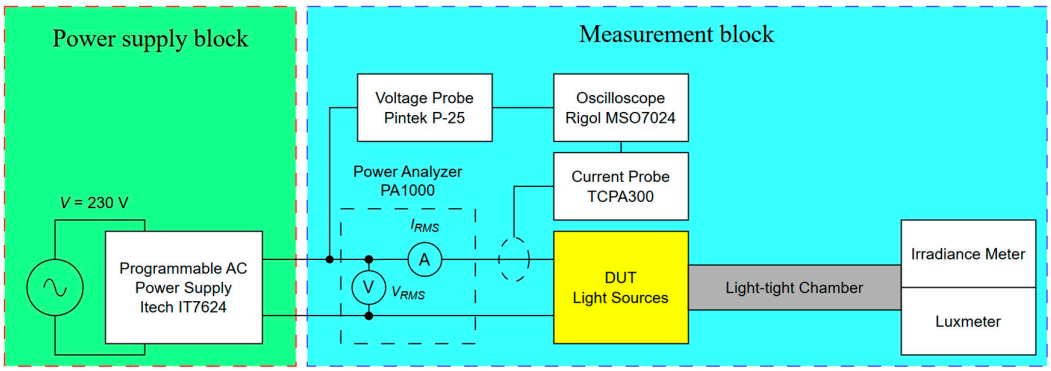

Figure 1. Diagram of the measuring set-up.

The measuring set-up consists of two blocks: a power supply block and a measuring block. The first one contains a programmable AC power supply IT7624 manufactured by ITECH (Zhonghe, New Taipei City, Taiwan) [25]. It has a maximum output apparent power of S = 1.5 kVA and a maximum effective voltage value of V_{inRMS} = 300 V. Among other things, it allows the voltage shape and amplitude to be changed, as well as the power factor (PF) to be measured. The maximum THD_V value is 0.5% for a mains frequency of f_{line} = 50 Hz. The data was recorded using the IT9000 application, version 1.0.0.9 [26].

The measurement block includes a Rigol MSO7024 oscilloscope (Suzhou, China) with a maximum sampling frequency of 10 GSa/s. The embedded software installed in it, extended with the RIGOL DS7000-PWR option, enables power analysis based on voltage and current waveforms. Using these, the oscilloscope automatically determines the power waveform $p(t)$ as the product of instantaneous current and voltage values, as well as the values of active power P, reactive power Q, apparent power S and phase shift φ [27]. A Tektronix TCPA300 current probe (Beaverton, OR, USA) was used to record current waveforms $i(t)$, while a Pintek DP-25 differential voltage probe (Shulin, New Taipei City, Taiwan) was used to record voltage waveforms $v(t)$ [28,29].

The PA1000 power analyser manufactured by Tektronix enabled the reading of effective values of voltage V_{inRMS}, current I_{inRMS}, and power [30]. It also allowed the determination of the Fourier transform (FFT) of current and voltage, which enabled the determination of the amplitudes and phases of individual harmonics and the values of the THD_V voltage total harmonic distortion and THD_I current total harmonic distortion [31]. The PWRVIEW application, version 3.1.0, enabled partially automated spectrum reading [32].

The power supply outputs were connected directly to the E27 socket, in which the light sources under consideration were placed. The tested light sources were placed inside a light-tight measuring track with a length of 50 cm. At the other end, a Delta OHM HD2302.0 exitance meter manufactured by Senseca (Nerviano, Italy) and an L-200P luxmeter with a P-200 panel manufactured by Sonopan (Białystok, Poland) were placed [33,34]. Using these instruments, it was possible to measure the values of excitement I_e and illuminance E.

The manufacturer of the IT7624 programmable AC source specifies the uncertainty of the built-in voltmeter as 0.2% of the reading and 0.2% of the total measurement range [25]. The PA1000 power analyzer, on the other hand, has a measurement uncertainty for effective voltage and current values of 0.04% of reading and 0.04% of the measurement range. The power measurement uncertainty is 0.075% of reading and 0.075% of the measurement range. For the power factor, it depends on the

 doi:10.20944/preprints202603.1372.v1

phase shift between voltage and current and is at least 0.002. The uncertainty for the measurement of effective values of voltage harmonic amplitudes is at least 0.05 V and 0.02% of the reading and 0.1% of the measurement range, and depends on the frequency of the measured voltage. For the effective amplitudes of current harmonics, it is 0.2% of the reading and 0.1% of the range, and additionally depends on the voltage amplitude and the impedance of the external shunt [30]. The measurement uncertainty of the exitance meter is 0.5%, while for the lux meter it is 2.0% for temperatures from 10 to 40 °C [33,34].

The power factor *PF* is defined as the quotient of active power *P* and apparent power *S* [35]. Its measurement was made possible by the IT7624 power supply. It uses instantaneous and effective values of voltage and current [36]:

$$PF = \frac{1}{T} \cdot \frac{\int_0^T v(t) \cdot i(t) dt}{V_{inRMS} \cdot I_{inRMS}} \tag{1}$$

where T denotes the waveform period, $v(t)$ and $i(t)$ denote the instantaneous values of voltage and current, V_{inRMS} and I_{inRMS} denote their effective values. The level of current distortion is characterized by the waveforms of current $i(t)$ and the total harmonic distortion coefficient THD_I [37]. It is determined by the following formula [38,39]:

$$THD_I = \sqrt{\frac{\sum_{k=2}^{n} I_k^2}{\sum_{k=1}^{n} I_k^2}} \cdot 100\% \tag{2}$$

where I_k denotes the effective value of the *k-th* harmonic of the supply current, and n denotes the number of harmonics (in this case, $n = 50$). Similarly, the total harmonic distortion for THD_V voltage can be determined:

$$THD_V = \sqrt{\frac{\sum_{k=2}^{n} V_k^2}{\sum_{k=1}^{n} V_k^2}} \cdot 100\% \tag{3}$$

where V_k denotes the effective value of the *k-th* harmonic of the supply voltage, and n again denotes the number of harmonics ($n = 50$). The uncertainty of measuring total harmonic distortion coefficient can be determined using the total differential method based on the effective values of individual harmonics and the uncertainty of the PA1000 power analyzer [40]. It is described by the following formula:

$$\Delta THD_I = \frac{I_1}{THD_I} \cdot \sqrt{\frac{I_1 \cdot \sum_{k=2}^{n} (I_k \cdot \Delta I_k) + \Delta I_1 \cdot \sum_{k=2}^{n} I_k^2}{\left(\sum_{k=1}^{n} I_k^2\right)^2}} \tag{4}$$

where ΔI_k denotes the measurement uncertainty of the effective value of the *k-th* harmonic of the supply current. Similarly, the uncertainty can be determined for the total harmonic distortion voltage (THD_V) coefficient:

$$\Delta THD_V = \frac{V_1}{THD_V} \cdot \sqrt{\frac{V_1 \cdot \sum_{k=2}^{n} (V_k \cdot \Delta V_k) + \Delta V_1 \cdot \sum_{k=2}^{n} V_k^2}{\left(\sum_{k=1}^{n} V_k^2\right)^2}} \tag{5}$$

where ΔV_k denotes the measurement uncertainty of the effective value of the *k-th* voltage harmonic. To determine the active power *P* value, samples of power waveforms $p(t)$ were used, and then the average active power *P* values were determined as integrals of these waveforms over time:

 doi:10.20944/preprints202603.1372.v1

$$P = \frac{1}{T}\int_0^T p(t)dt = \sum_{k=2}^{n} \frac{[t(k)-t(k-1)]\cdot[p(k)-p(k-1)]}{2T} \quad (6)$$

where n denotes the number of samples, $t(k)$ denotes the time of sampling the k-th sample, and $p(k)$ denotes the instantaneous power value for time $t(k)$.

4. Results

The measuring set-up described in Chapter 3 allowed for the determination of parameters describing power quality. The light sources were powered using a programmable AC power supply IT7624 with a sinusoidal voltage with adjustable effective value V_{inRMS} and a constant mains frequency f_{line} = 50 Hz. Figures 2 to 8 show the measured and calculated power supply parameters of selected light sources for a sinusoidal supply voltage waveform with a mains frequency f_{line} = 50 Hz.

4.1. The Influence of the Effective Value of the Supply Voltage on the Operating Parameters of the Tested Light Sources

Figure 2 shows the relationship between the effective value of the supply current I_{inRMS} and the effective value of the supply voltage V_{inRMS}. This relationship was determined using a Tektronix PA1000 power analyzer.

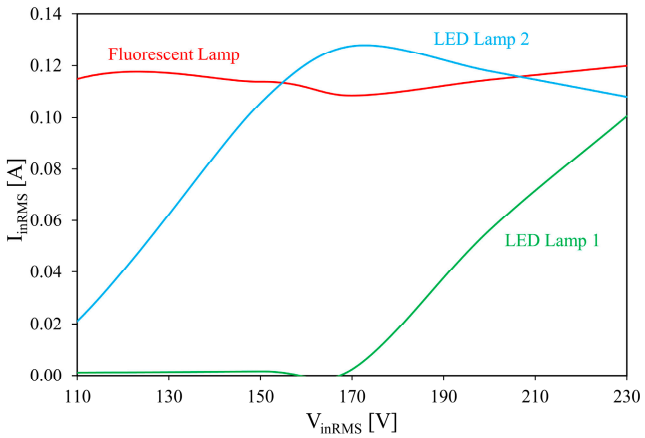

Figure 2. Measured dependence of the effective value of the supply current I_{inRMS} on the effective value of the supply voltage V_{inRMS} for the tested light sources.

When analyzing this relationship, a high degree of correlation with the apparent S, active P and reactive Q power relationships can be observed, including the same limit values above which the current values for both LED lamps increase rapidly. The effective value of the supply current for LED Lamp 2 reaches a maximum of I_{inRMS} = 130 mA for a supply voltage of V_{inRMS} = 170 V.

Figure 3 shows the relationship between reactive power Q and active power P for a sinusoidal supply waveform.

Based on the relationship shown in Figure 3, it can be seen that the active power P increases almost linearly for all three selected light sources. The highest active power values P for the same reactive power value Q were obtained mainly for Fluorescent Lamps, while the lowest were obtained for LED Lamp 1. The reactive power was greater than the active power across the entire range of values for all three light sources tested.

 doi:10.20944/preprints202603.1372.v1

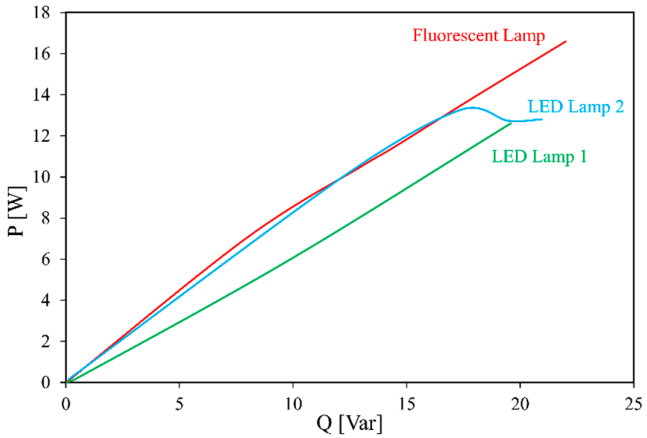

Figure 3. Measured relationship between reactive power *Q* and active power *P* for the tested light sources.

Figures 4 to 5 describe the relationship between the power factor *PF* (Figure 4) and the total harmonic distortion for THD_V voltage (Figure 5a) and THD_I current (Figure 5b) as a function of the supply voltage V_{inRMS}. The *PF* values were measured using the internal measurement system of the IT7624 AC power supply.

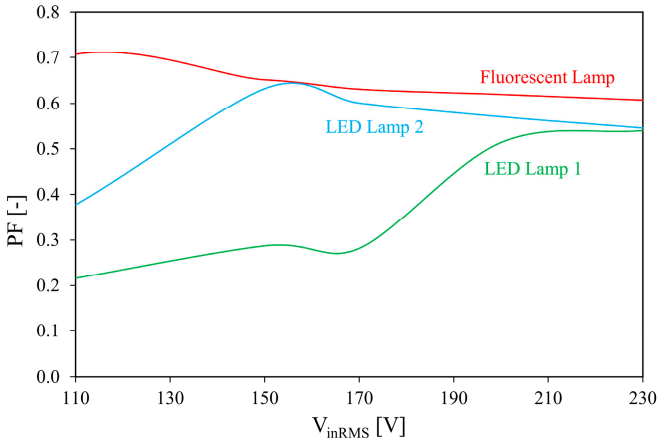

Figure 4. Measured dependence of the power factor *PF* on the effective value of the supply voltage V_{inRMS} for the tested light sources.

Based on the determined relationship, it can be seen that the *PF* values are generally low. In the case of Fluorescent Lamps, the maximum *PF* = 0.7 is already achieved for an effective voltage value of V_{inRMS} = 110 V, while for LED Lamps 2, the maximum *PF* = 0.65 is achieved for V_{inRMS} = 160 V. For LED Lamp 1, the power factor stabilizes at *PF* = 0.55 for an effective supply voltage above V_{inRMS} = 200 V. The obtained power factor *PF* value meets the requirements of the international standard IEC 61000-3-2:2018 for exceeding *PF* = 0.5 for voltages above V_{inRMS} = 80 V for Fluorescent Lamp, V_{inRMS} = 200 V for LED Lamp 1 and V_{inRMS} = 130 V for LED Lamp 2.

Figure 5 shows the relationship between the THD_V voltage total harmonic distortion coefficient and THD_I current total harmonic distortion coefficients and the effective supply voltage V_{inRMS} value. They were calculated using formulas (2) and (3) based on the effective amplitudes of the first fifty harmonics determined using a Tektronix PA1000 power analyzer.

 doi:10.20944/preprints202603.1372.v1

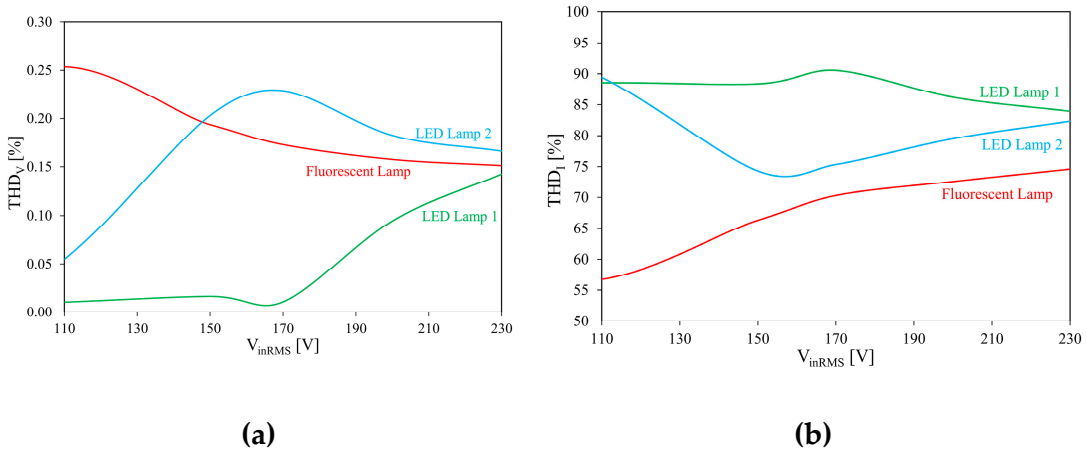

Figure 5. Calculated dependencies of THD_V (a) and THD_I (b) total harmonic distortion coefficients on the effective value of the supply voltage V_{inRMS} for the tested light sources.

When analyzing Figure 5, it can be seen that the THD_V values for all three light sources are low and do not exceed 8%, and are therefore lower than the upper limit described in IEC 61000-3-3:2013 and EN 50160 standards and 5% described in IEEE 519-2022 standard. The highest THD_V value of 0.25% is achieved for an effective supply voltage of V_{inRMS} = 110 V for Fluorescent Lamps and THD_V = 0.23% for V_{inRMS} = 165 V for LED Lamps 2. The value of this parameter was lowest for LED Lamp 1. The $THD_I(V_{inRMS})$ relationship indicates very high harmonic content values for the supply current. It was lowest for Fluorescent Lamp. Depending on the light source, the THD_I value ranged from 55% to 95%, thus never meeting the requirement of not exceeding the limit value of 23% described in the IEC 61000-3-2:2018 standard.

Figure 6 shows the relationship between the normalized value of the exitance I_e and the effective value of the supply voltage V_{inRMS}. These were measured using an appropriate radiometric probe placed 50 cm from the light source using a light-tight measuring track.

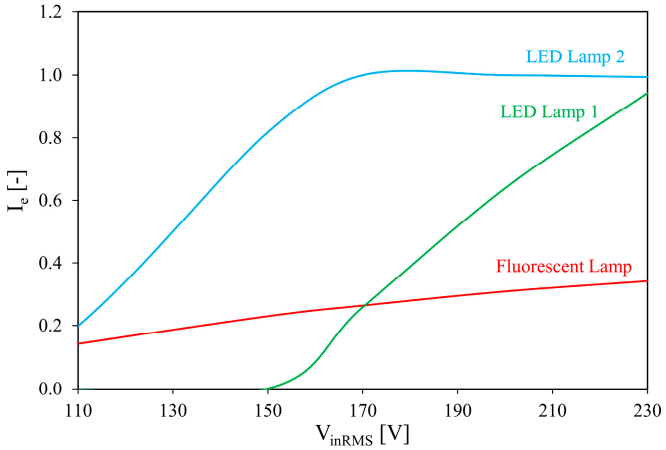

Figure 6. The measured dependence of the normalized value of the exitance I_e on the effective value of the supply voltage V_{inRMS} for the tested light sources.

When analyzing the relationship shown in Figure 6, it can be seen that the Fluorescent Lamp has a significantly lower normalized exitance value I_e compared to other light sources. For effective supply voltages V_{inRMS} below a certain threshold, the exitance of LED lamp 1 was close to zero, while above the threshold it increased rapidly. This voltage was V_{inRMS} = 150 V. In the case of LED lamp 2,

 doi:10.20944/preprints202603.1372.v1

the rate of increase decreased for V_{inRMS} > 150 V, and for V_{inRMS} > 200 V, the exitance value was relatively constant.

Figure 7 shows the waveforms of the supply current I_{in} (Figure 7a) and the waveforms of the power $p(t)$ (Figure 7b), while Figure 8 shows the amplitude spectrum of the current drawn from the power grid (Figure 8a) and the phase spectrum (Figure 8b). The amplitude spectrum of the current drawn from the power grid is presented in the form of histograms showing the amplitude and phase values of the first thirty harmonics. The amplitude spectrum is presented as values normalized to the first harmonic.

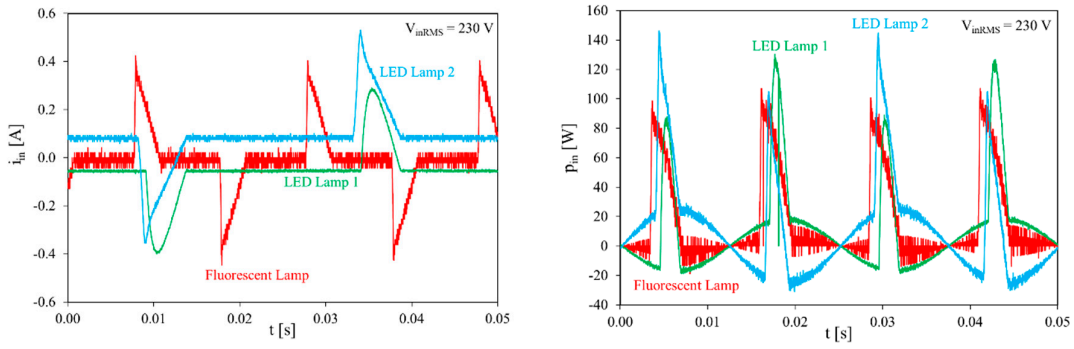

(a) **(b)**

Figure 7. Measured waveforms of current i_{in} (a) and power p_{in} (b) when powered by a sinusoidal waveform for the tested light sources.

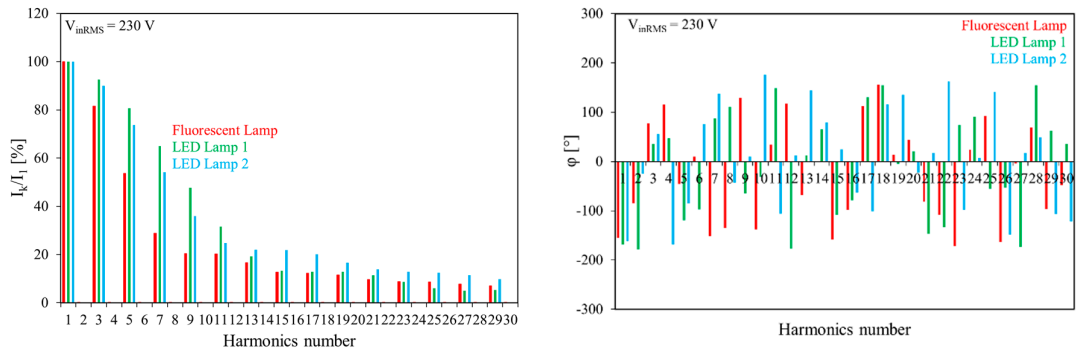

(a) **(b)**

Figure 8. Measured amplitude (a) and phase (b) spectra of the current I_{in} drawn from the power grid when supplied with a sinusoidal waveform for the tested light sources.

When analyzing Figure 7a, it can be seen that the waveforms of the current drawn from the power grid deviate significantly from a sinusoidal shape, which is a consequence of high levels of harmonic distortion. Much stronger distortions are observed for LED lamps. The peak-to-peak current value was approximately I_{pp} = 800 mA for the fluorescent lamp and approximately I_{pp} = 200 mA for both LED lamps. In their case, the presence of a constant current component was also observed, with an absolute value of approximately I_{in} = 60 mA for LED Lamp 1 and I_{in} = 80 mA for LED Lamp 2.

 doi:10.20944/preprints202603.1372.v1

An analysis of Figure 7b shows that current distortions affect the quality of energy consumed from the power grid, which is confirmed by the *p(t)* waveform, whose shape does not resemble a sine wave. The peak-to-peak power value was P_{pp} = 120 W for Fluorescent Lamp, P_{pp} = 150 W for LED Lamp 1 and P_{pp} = 180 W for LED Lamp 2. The occurrence of negative fragments of the *p(t)* waveform indicates a clear phase shift between the current and voltage waveforms.

The relationship shown in Figure 8a indicates a very high level of current distortion, which is confirmed by the very high normalized values of individual harmonics. No even harmonics with high amplitudes were recorded. The effective values of the spectral stripes for fluorescent lamps were generally lower than for LED lamps. None of the light sources considered met the requirements described in IEC 61000-3-2:2018. It is also required that the third harmonic does not exceed the normalized value of I_3 = 21.6% I_1, which is confirmed by the values of the first harmonics, which are I_3 = 81.54% I_1 for Fluorescent Lamp, I_3 = 92.61% I_1 for LED Lamp 1 and I_3 = 90% I_1 for LED Lamp 2.

Based on the histogram shown in Figure 8b, significant variability in phase shift between individual current harmonics was observed. The distribution obtained is not orderly. Therefore, designing a system that shifts the phase of harmonic currents may be difficult.

4.2. The Influence of Supply Voltage Shape on the Operating Parameters of Selected Light Sources

The second part of the study determined the impact of the supply voltage waveform on the quality of electricity, distortion and optical parameters of the light sources under consideration. Three supply waveforms were considered: sinusoidal, rectangular and triangular with a mains frequency of f_{line} = 50 Hz. The measured and calculated relationships are presented in Figures 9 to 17. The results of the study presented in this section provide a basis for assessing the correct operation of light sources in the event of distortions in the power grid causing the mains voltage to deviate from a sinusoidal waveform [41,42]. As is known from [43], an increased level of harmonic distortion can lead to a noticeable reduction in luminous efficiency.

Figure 9 shows the relationship between the effective value of current I_{inRMS} and the effective value of voltage V_{inRMS} for different supply voltage waveforms. Figure 10 shows the relationship between active power *P* and reactive power *Q*, while Figures 11 and 12 show the relationships between the power factor *PF* and the voltage total harmonic distortion coefficient THD_V and current total harmonic distortion coefficient THD_I, and the effective value of the supply voltage V_{inRMS}, for different supply voltage waveforms. The solid lines indicates the relationship for a sinusoidal voltage, the dashed lines for a square wave voltage, and the dotted lines for a triangular wave voltage.

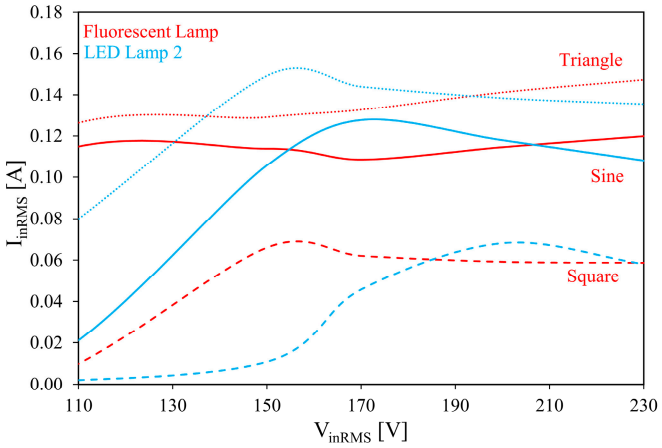

Figure 9. Measured relationship between the effective value of current I_{inRMS} and the effective value of supply voltage V_{inRMS} for different supply waveforms for fluorescent lamps and LED lamps 2.

Analyzing Figure 9, it can be seen that the highest current (up to I_{inRMS} = 147 mA) was obtained for a fluorescent lamp powered by a triangle wave voltage at V_{inRMS} = 230 V, lower (up to I_{inRMS} = 120

 doi:10.20944/preprints202603.1372.v1

mA) for a sinusoidal wave voltage, and lowest (up to I_{inRMS} = 66 mA) for a square wave voltage. A similar relationship exists between the characteristics for different voltage, although for voltage values above V_{inRMS} = 150 V for a triangular wave voltage, V_{inRMS} = 170 V for a sinusoidal wave voltage and V_{inRMS} > 200 V for a square wave voltage, a decrease in the effective current value is observed with increasing voltage.

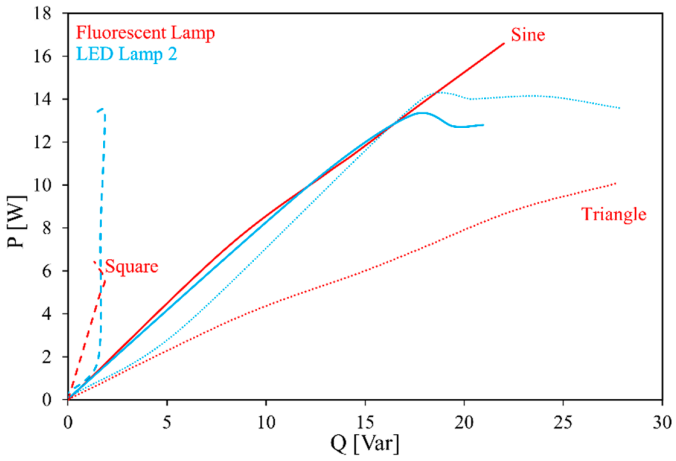

Figure 10. Measured relationship between active power P and reactive power Q for Fluorescent Lamp and LED Lamp 2.

When analyzing Figure 10, it can be seen that for sinusoidal and triangular wave voltage supplies, the active power *P* was lower than the reactive power *Q*. For Fluorescent Lamps, the relationship is almost linear, while for LED Lamps 2, it stabilizes relatively above the reactive power Q = 17 Var. For square wave voltage supply, the lowest P and Q values are obtained, but the active power was much higher than the reactive power. Supplying the considered light sources with square wave voltage may be more energy efficient.

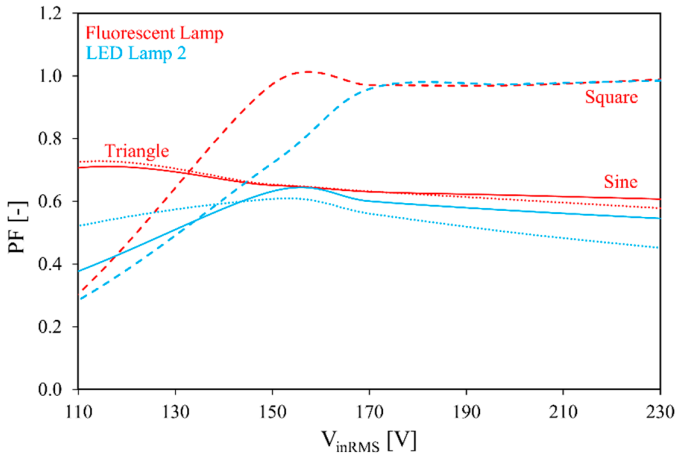

Figure 11. Measured dependence of the power factor *PF* on the effective value of the supply voltage V_{inRMS}, for different supply voltage waveforms, for Fluorescent Lamp and LED Lamp 2.

Based on the relationship shown in Figure 11, it can be seen that supplying the Fluorescent Lamp with a square wave voltage greatly increases the power factor for V_{inRMS} > 150 V, where the power factor is *PF* > 0.97. For V_{inRMS} = 230 V, it reaches a maximum value of *PF* = 0.989. For sinusoidal and triangular waveforms voltages, the power factor *PF* values for the Fluorescent Lamp are comparable

 doi:10.20944/preprints202603.1372.v1

and do not exceed $PF = 0.7$ across the entire voltage range. In the case of LED Lamp 2 powered by a square waveform voltage, a linear increase in the power factor to $PF = 0.95$ is observed at an effective supply voltage $V_{inRMS} = 170$ V. For $V_{inRMS} = 230$ V, the maximum value of $PF = 0.985$ is again reached. In the case of sinusoidal wave and triangular wave voltage supply, the power factor never exceeded $PF = 0.64$.

Figure 12 shows the relationship between THD_V and THD_I and the effective value of the supply voltage V_{inRMS} for Fluorescent Lamp and LED Lamp 2. They were calculated using formulas (2) and (3) and the effective values of the amplitudes of the first fifty harmonics, recorded using a Tektronix PA1000 power analyzer with the PWRVIEW application.

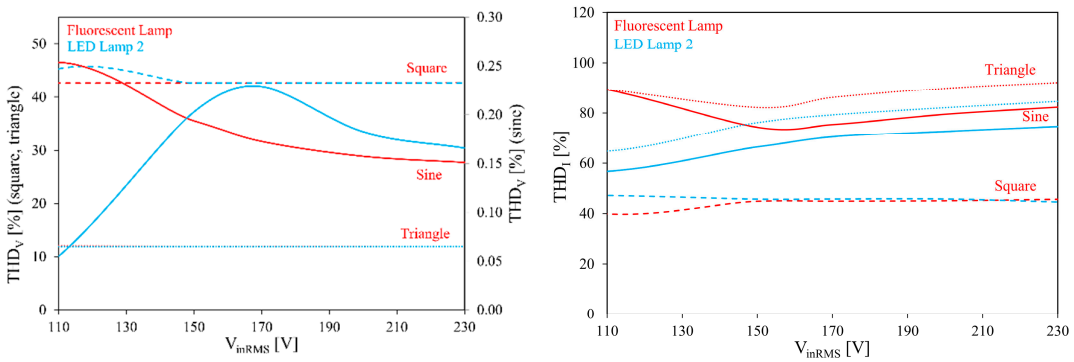

Figure 12. Calculated relationship between total harmonic distortion coefficients for THD_V voltage and THD_I current and the effective value of supply voltage V_{inRMS} for different supply voltage waveforms, for Fluorescent Lamp (a) and LED Lamp 2 (b).

When analyzing Figure 12a, it can be seen that not exceeding the upper limit of the supply voltage harmonic content factor $THD_V = 8\%$ described in standards IEC 61000-3-3:2013 and EN 50160, and $THD_V = 5\%$ described in the IEEE 519-2022 standard, only guarantees a sinusoidal waveform voltage supply. For a triangular waveform voltage, the THD_V coefficient values were 12% across the entire supply voltage range, and 42.6% for a rectangular waveform voltage. The THD_I coefficient values were highest for the triangular waveform voltage, lower for the sinusoidal waveform voltage, and lowest for the rectangular waveform voltage. However, they were not lower than $THD_I = 44\%$, which is higher than the upper limit of $THD_I = 23\%$ specified in the IEC 61000-3-2:2018 standard. Therefore, the requirements specified in this standard were not met.

When analyzing Figure 12b, similar characteristics can be observed for LED Lamp 2. The THD_V values obtained for LED Lamp 2 were comparable to those for Fluorescent Lamp, although this parameter only stabilized above the effective supply voltage $V_{inRMS} = 150$ V in the case of a square waveform voltage. The THD_I values were also comparable to those of Fluorescent Lamp, thus not complying with the IEC 61000-3-2:2018 standard.

Figure 13 shows the relationships normalized to the maximum exitance I_e from the effective value of the supply voltage V_{inRMS}.

Analyzing Figure 13, it can be seen that across the entire range of changes in the effective value of the supply voltage V_{inRMS}, the exitance I_e for the Fluorescent Lamp takes on the highest values when supplied with a triangular waveform voltage, lower values for a sinusoidal waveform voltage, and the lowest values for a square waveform voltage. Analyzing the relationships for LED Lamp 2, it can be seen that for all three supply voltage waveforms, significantly higher exitance values are achieved compared to Fluorescent Lamp. In the case of a triangular voltage supply, it is always higher than for a

 doi:10.20944/preprints202603.1372.v1

sinusoidal voltage supply. For an effective supply voltage V_{inRMS} > 175 V, the highest exitance values are achieved for square waveform voltage, while below this voltage value, the exitance value is the lowest.

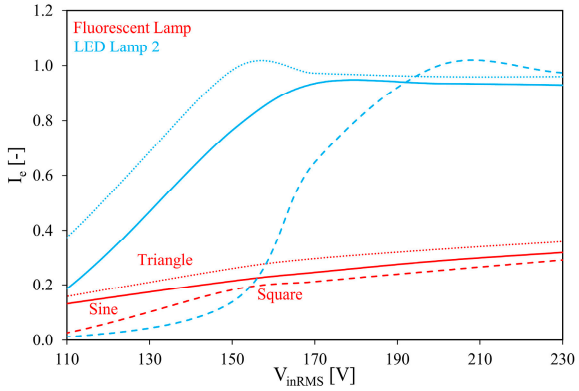

Figure 13. Measured dependence of normalized exitance I_e on the effective value of the supply voltage V_{inRMS}, for different supply voltage waveforms, for Fluorescent Lamps and LED Lamps 2.

Figures 14–17 show the waveforms of current *i(t)* and power *p(t)*, as well as the spectrum describing the effect of the supply voltage waveform on current distortion. The measurements were made for a supply voltage RMS value of V_{inRMS} = 230 V and a mains frequency of f_{line} = 50 Hz. Each harmonics visible in the presented spectra are normalized to the first harmonic.

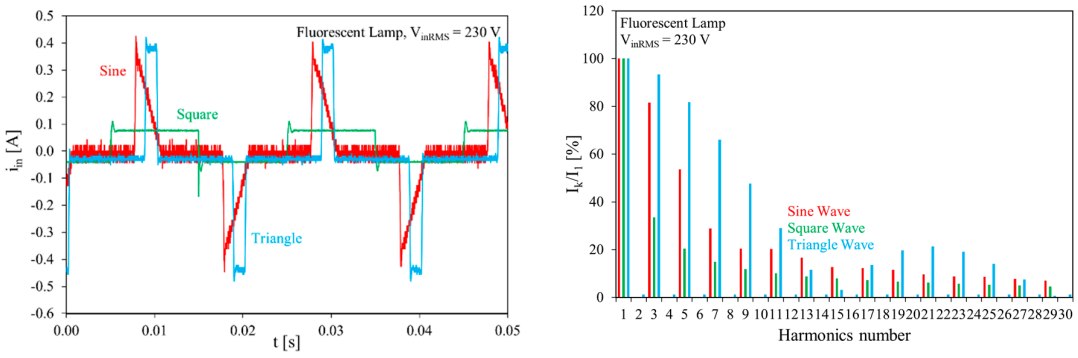

(a) **(b)**

Figure 14. Measured waveforms of current I_{in} for different shapes of supply voltage to a fluorescent lamp (a) and their spectra normalized to the first harmonic (b).

Analyzing Figure 14a, in the case of supplying the Fluorescent Lamp with sinusoidal and triangular waveforms voltage, a high level of current distortion can be observed. In the case of rectangular waveform voltage, it was significantly lower. The peak-to-peak value of the supply current for the sinusoidal waveform voltage was approximately I_{pp} = 800 mA, and for the square waveform voltage only about 170 mA.

Figure 14b shows very high levels of odd harmonics for fluorescent lamps, particularly when powered by a triangular waveform voltage. Only in this case were even harmonics with values above 1% I_1 observed. The lowest values of individual harmonics were obtained for square waveform voltage. Regardless of the voltage shape, however, it was not possible to meet the harmonic requirements described in IEC 61000-3-2:2018.

 doi:10.20944/preprints202603.1372.v1

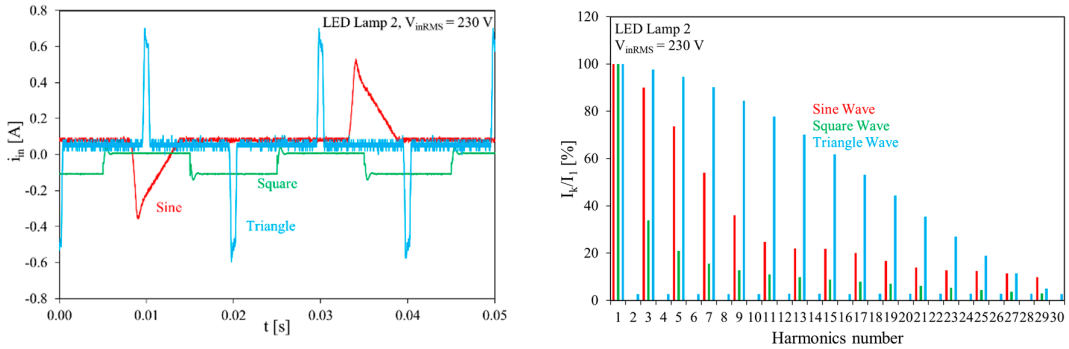

(a) **(b)**

Figure 15. Measured waveforms of the supply current I_{in} for different shapes of the supply voltage of LED Lamp 2 (a) and their spectra normalized to the first harmonic (b).

Figure 15a shows the waveforms of the I_{in} current for LED Lamp 2 powered by voltages of different shapes. The effect of voltage shape is more pronounced for Fluorescent Lamp. The highest level of distortion is observed for sinusoidal waveform voltage, where only one half-wave per period is observed, and the peak-to-peak value of the supply current was I_{pp} = 400 mA. In the case of triangular waveform voltage, the supply current period contained two half-waves with a peak-to-peak value of I_{pp} = 1.3 A, but its shape was far from triangular. The least distorted waveform (with I_{pp} = 100 mA) was obtained for rectangular waveform voltage. The value of the constant component of the supply current for LED Lamp 2 does not depend on the shape of the voltage and is I = 80 mA.

Figure 15b shows the harmonic spectrum for LED Lamp 2, for the same supply voltage waveforms. They show a high degree of similarity to the spectrum determined for the Fluorescent Lamp. Once again, an increase in the effective harmonic values, including even harmonics, was observed for the triangular waveform voltage relative to the sinusoidal waveform voltage, and a decrease for the rectangular waveform voltage.

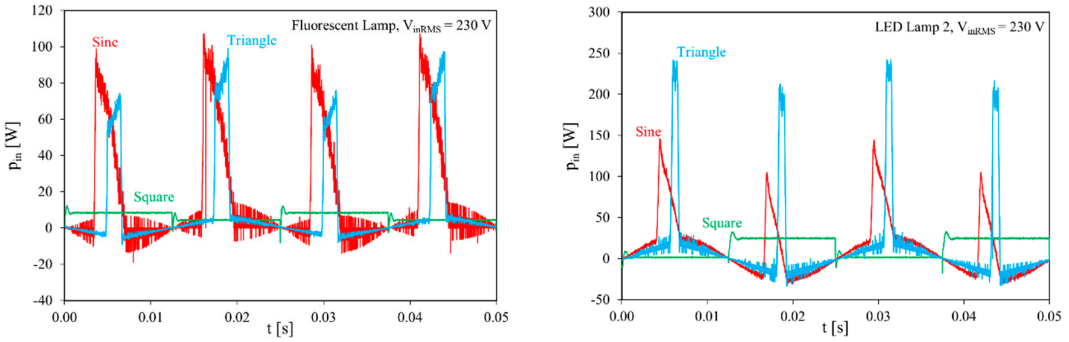

(a) **(b)**

Figure 16. Measured waveforms of instantaneous power p for different supply voltage waveforms for Fluorescent Lamp (a) and LED Lamp 2 (b).

When analyzing Figure 16a, it was observed that the level of supply current distortion again affected the deterioration of the power supply quality. This is indicated by the instantaneous power

 doi:10.20944/preprints202603.1372.v1

waveforms *p(t)* obtained for the Fluorescent Lamp, which do not resemble a sine wave, square wave (constant component) or triangular wave. The peak-to-peak value of instantaneous power was p_{pp} = 110 W for sinusoidal waveform voltage, p_{pp} = 10 W for square waveform voltage, and p_{pp} = 100 W for triangular waveform voltage. The lowest level of distortion was again observed for square waveform voltage supply.

When analyzing Figure 16b, it can be seen that the supply current distortions introduced by LED Lamp 2 lead to an even greater deterioration in power quality. The obtained waveforms deviate even more from the supply waveforms, with the instantaneous power waveform for the square waveform voltage being the least distorted again. A significantly higher phase shift value compared to the Fluorescent Lamp can also be observed. The peak-to-peak instantaneous power value was p_{pp} = 180 W for sinusoidal waveform voltage, p_{pp} = 30 W for square waveform voltage, and p_{pp} = 270 W for triangular waveform voltage. Such high peak-to-peak power values result from a strong phase shift, leading to the coexistence of high instantaneous voltage and current values.

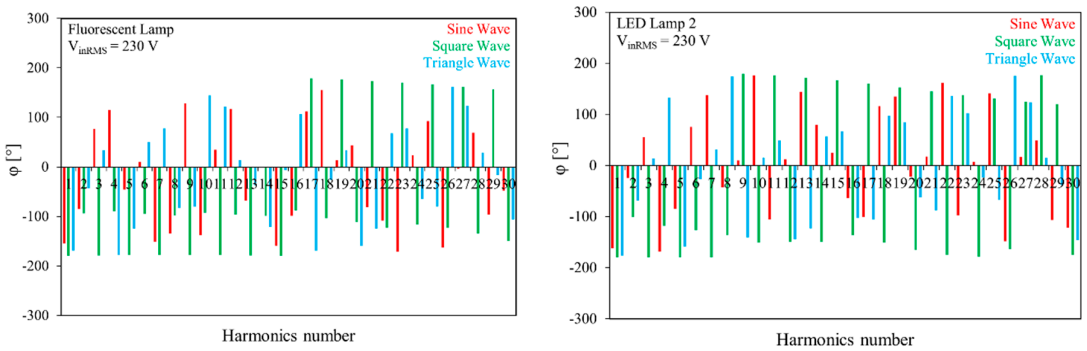

(a) **(b)**

Figure 17. Measured phase spectrum of the supply current for different supply voltage waveforms, for Fluorescent Lamp (a) and LED Lamp 2 (b).

When analyzing Figure 17a, one can observe a clear variability in the phase shift values between individual current harmonics for Fluorescent Lamps. For square waveform voltage supply, the distribution of these shifts is relatively orderly, with many consecutive odd harmonics assuming similar values. In the case of sinusoidal and triangular waveform voltages, the distribution is not very orderly.

Figure 17b shows the distribution of phase shifts of supply current harmonics for LED Lamp 2. In the case of square waveform voltage, a deterministic pattern was again observed. For sinusoidal and triangular waveform voltages, no patterns were observed again, which hinders further shifting of harmonics by power electronic circuits.

The results presented in Figures 14 to 17 indicate a slight improvement in power quality when the power supply voltage waveform is changed to rectangular or triangular shape. However, only the rectangular waveform leads to a reduction in harmonic distortion.

5. Conclusions

The article describes the results of measurements of the electrical and photometric characteristics of a fluorescent lamp and two LED light sources. The characteristics were measured in the range of effective supply voltage V_{inRMS} from 110 to 230 V, with sinusoidal, rectangular and triangular waveforms. The appropriate supply voltage waveforms were obtained using a programmable AC power supply. Waveforms and spectra describing current distortion and power quality were also determined.

 doi:10.20944/preprints202603.1372.v1

Based on the determined power characteristics, it was found that semiconductor light sources manufactured using different technologies by different manufacturers may have different relationships between active P and reactive Q power . Some of them may resemble the power characteristics of fluorescent lamps. In the case of semiconductor light sources, high reactive power values are observed, which may lead to higher electricity consumption. This phenomenon can be reduced by supplying the light source with a square waveform voltage. A deterministic relationship between active power and exitance has also been observed, on the basis of which it has been concluded that exitance increases with active power, both for LED lamps and fluorescent lamps. Powering an LED lamp with a triangular or square waveform voltage can increase the ratio of active to reactive power and also increase the value of the exitance.

Both fluorescent lamps and LED lamps are characterized by a relatively low power factor (PF), which, when powered by a sinusoidal waveform voltage, never exceeded 0.7 for fluorescent lamps and 0.65 for LED lamps. Based on measurements taken for other waveforms, it was found that a rectangular power supply waveform can increase the power factor PF to even above 0.98.

Fluorescent and LED lamps are characterized by high harmonic current distortion, as confirmed by measurement results showing THD_I values ranging from 55% to 95%. The use of a square waveform supply voltage can slightly reduce the THD_I value to 45%. The use of triangular waveform voltage is not conducive to THD_I reduction.

The use of an oscilloscope with a power analysis option allowed us to determine the waveforms of current and power. The shapes of these waveforms deviated significantly from the expected ones, which corresponds to a high level of distortion. Powering fluorescent and LED lamps using a square waveform voltage leads to both an improvement in the shape of the current and power waveforms and a reduction in the level of harmonic distortion. A triangular waveform voltage improves the shape of the current and power waveforms to a much lesser extent and also leads to an increase in the level of harmonic distortion.

The PA1000 power analyzer enabled spectral analysis of the power supply voltage. The phase spectrum determined for fluorescent lamps powered by square waveform voltage is characterized by high determinism, thus demonstrating high potential for modelling these distortions, which may translate into the development of appropriate phase-shifting transformers.

The results obtained may be useful for designers of power electronic circuits for semiconductor light sources powered from the mains.

Author Contributions: Conceptualization, P.P. and T.L.; methodology, P.P., T.L. and K.G.; validation, P.P., T.L. and K.G.; investigation, P.P. and T.L.; resources, P.P. and K.G.; writing—original draft preparation, P.P. and T.L.; writing—review and editing, P.P., K.G.; visualization, P.P. and T.L.; supervision, K.G. All authors have read and agreed to the published version of the manuscript.

Funding: This research received no external funding.

Data Availability Statement: The presented experimental data can be made available on request.

Conflicts of Interest: The authors declare no conflicts of interest.

Abbreviations

The following abbreviations are used in this manuscript:

AC	Alternating Current
DC-DC	Direct Current to Direct Current
FFT	Fast Fourier Transform
GaN	Gallium Nitride
GaN-FET	Gallium Nitride Field Effect Transistor
InGaN	Indium and Gallium Nitride
LED	Light Emitting Diode
PF	Power Factor

 doi:10.20944/preprints202603.1372.v1

PFC	Power Factor Correction
THD	Total Harmonic Distortion
THD_I	Total Harmonic Distortion of Current
THD_V	Total Harmonic Distortion of Voltage

References

1. Van Gompel, S. Light Bulb. In *A History of Intellectual Property in 50 Objects*; Op den Kamp, C., Hunter, D., Eds.; Cambridge University Press: Cambridge, United Kingdom, 2019; pp. 105–112, doi: https://doi.org/10.1017/9781108325806.013
2. Kykta, M. The Incandescent Light Bulb and the Mystery of the Centennial Bulb. *Information Display* **2021**, *2021 May/June*, pp. 1-5.
3. Pust, P.; Schmidt P. J., Schnick, W. A revolution in lighting. *Nature materials* **2015**, *14*(5), pp. 454-458.
4. Gayral, B. LEDs for lighting: Basic physics and prospects for energy savings. *Comptes Rendus. Physique* **2017**, *18*(7-8), pp. 453-461, doi: http://dx.doi.org/10.1016/j.crhy.2017.09.001
5. Pattison, P.M.; Hansen, M.; Tsao, J.Y., LED lighting efficacy: status and directions. *Comptes Rendus. Physique* **2018**, *19*(3), pp. 134-145, doi: https://doi.org/10.1016/j.crhy.2017.10.013
6. Virk, H.S. History of luminescence from ancient to modern times. *Defect and Diffusion Forum* **2015**, Vol. 361, pp. 1-13, doi: 10.4028/www.scientific.net/DDF.361.1
7. Fontoynont, Marc. LED lighting, ultra-low-power lighting schemes for new lighting applications. *Comptes Rendus. Physique* **2018,** *19.3 (2018)*, pp. 159-168.
8. Pulli, T.; Dönsberg, T.; Poikonen, T.; Manoocheri, F.; Kärhä, P.; Ikonen, E. Advantages of white LED lamps and new detector technology in photometry. *Light: Science & Applications* **2015**, *4*(9), e332, doi: doi:10.1038/lsa.2015.105
9. Mohamed Junaid, K.A.; Sukhi, Y.; Anjum, N.; Jeyashree, Y.; Fayaz Ahamed, A.; Debbarma, S.; Chaudhary, G.; Priyadarshini, S.; Shylashree, N.; Garg, S.; Kumar, M.; Nath, V. PV-based DC-DC buck-boost converter for LED driver. *e-Prime-Advances in Electrical Engineering, Electronics and Energy* **2023**, 5(2023):100271, doi: https://doi.org/10.1016/j.prime.2023.100271
10. Cheng, C.A.; Cheng, H.L.; Chang, C.H.; Chang, E.C.; Kuo, Z.Y.; Lin, C.K.; Hou, S.H. A novel AC-DC LED integrated streetlight driver with power-factor-correction and soft-switching functions. In Proceedings of *2021 IEEE International Future Energy Electronics Conference (IFEEC)*, Taipei, Taiwan, 16-19 November 2021.
11. Adhigunarto, S.; Mulyana, E.; and Surya, W. The Analysis of Harmonics on LED Lamps. *IOP Conf. Ser.: Mater. Sci. Eng*. **2018**, 384 (2018) 012061, doi: https://doi.org/10.1088/1757-899X/384/1/012061
12. Coutinho, R.P.; de Souza, K.C.; Antunes, F.L.; & Sá, E.M. Three-phase resonant switched capacitor LED driver with low flicker. *IEEE Transactions on Industrial Electronics* **2017**, *64*(7), pp. 5828-5837.
13. Pereira, A.M.E.; Teixeira, V.A.; Fortes, M.Z.; Tavares, G.M.; Ferreira, V.H. Power quality analysis of domestic lamps available in the Brazilian market. *WSEAS Trans. Circuits* **2015**, *14*, pp. 389-399.
14. dos Santos Oliveira, G.; de Oliveira, E.P.; da Silva, A.P.; de Moura Carvalho, C.C.M. Power quality of LED lamps. In Proceedings of *2016 17th International Conference on Harmonics and Quality of Power (ICHQP)*, Belo Horizonte, Minas Gerais, Brazil, 16-19 October 2016.
15. IEC 61000-3-2:2018 standard. Electromagnetic compatibility (EMC) – Part 3-2: Limits – Limits for harmonic current emissions (equipment input current ≤ 16 A per phase)
16. IEC 61000-3-3:2013 standard. Electromagnetic compatibility (EMC) – Part 3-3: Limits – Limitation of voltage changes, voltage fluctuations and flicker in public low-voltage supply systems, for equipment with rated current ≤ 16 A per phase and not subject to conditional connection
17. EN 50160 standard. Voltage characteristics of electricity supplied by public distribution systems
18. IEEE 519-2022 standard. IEEE Standard for Harmonic Control in Electric Power Systems
19. Anisah, S.; Fitri, R.; Taro, Z.; Wijaya, R.F. Comparison of Lighting Efficiency (Led-CFL) based on Environmentally Friendly Technology. *Journal of Applied Engineering and Technological Science (JAETS)* **2022**, *4*(1), pp. 568-577.

 doi:10.20944/preprints202603.1372.v1

20. Cenci, M.P.; Dal Berto, F.C.; Schneider, E.L.; Veit, H.M. Assessment of LED lamps components and materials for a recycling perspective. *Waste Management* **2020**, *107*, pp. 285-293, doi: https://doi.org/10.1016/j.wasman.2020.04.028
21. Castro I.; Vazquez A.; Arias M.; Lamar, D.G.; Hernando, M.M.; Sebastian, J. A review on flicker-free AC–DC LED drivers for single-phase and three-phase AC power grids. *IEEE Transactions on Power Electronics* **2019**, *34*(10), pp. 10035-10057, doi: https://doi.org/10.1109/TPEL.2018.2890716
22. ENERGY STAR® Program Requirements Product Specification for Luminaires (Light Fixtures). Available online: https://www.energystar.gov/sites/default/files/asset/document/Luminaires%20V2%200%20Final.pdf (accessed on 7 March 2026).
23. Skarżyński, K.; Wiśniewski, A. The reflections on energy costs and efficacy problems of modern LED lamps. *Energy Reports* **2024**, *12*, pp. 4926-4937, doi: https://doi.org/10.1016/j.egyr.2024.10.038
24. Górecki, K.; Ptak, P.; Heleniak, J. Badania zniekształceń prądu zasilającego i egzytancji energetycznej wybranych lamp. *Przegląd Elektrotechniczny* **2022**, *98*, pp. 90-93, doi: https://doi.org/10.15199/48.2022.09.18
25. Programmable AC Power Supply. Series IT7600 User's Manual. Available online: https://www.itechate.com/uploadfiles/2019/09/201909231256295629.pdf (accessed on 7 March 2026).
26. IT9000 Control Software. PV6400 User Manual. Available online: https://www.altoo.dk/cosmoshop/default/artikelpdf/IT-6400-SW_en.pdf?srsltid=AfmBOooHnR701rW0NSbtJoHQ7NbCEAwbAz-A9rpYe7RsDe7hE1brECg0 (accessed on 7 March 2026).
27. RIGOL User Guide. MSO7000/DS7000 Series Digital Oscilloscope. Available online: https://tw.rigol.com/tw/Images/DS7000UserGuideEN_tcm17-3987.pdf (accessed on 7 March 2026).
28. Tektronix TCPA300/400 Amplifiers & TCP300/400 Series AC/DC Current Probes. Instruction Manual. Available online: https://download.tek.com/manual/071118303.pdf (accessed on 7 March 2026).
29. DP-25/DP-50/DP-100 High Voltage Differential Probe. Instruction Manual. Available online: https://www.pintek.com.tw/customer/pintek/upload/DP-MANUAL.pdf (accessed on 7 March 2026).
30. PA1000. Single Phase AC/DC Power Analyzer Datasheet. Available online: https://www.testequipmenthq.com/datasheets/TEKTRONIX-PA1000-Datasheet.pdf (accessed on 7 March 2026).
31. Ptak, P.; Lorkowski, T.; Górecki, K. Influence of the Type of Load on Characteristics of a Dedicated USB PD Charging System—A Case Study. *Appl. Sci.* **2025**, 15, 5254, doi: https://doi.org/10.3390/app15105254
32. PWRVIEW Analysis Software - 64 Bit - V3.1.0 | Tektronix. Available online: https://www.tek.com/en/support/software/application/pa1000-software-pwrview-64 (accessed on 7 March 2026).
33. Photo-radiometer HD2302.0. Operating manual. Available online: https://environmental.senseca.com/wp-content/uploads/document/DeltaOHM_HD2302.0_manual_ENG.pdf (accessed on 7 March 2026).
34. The family of L-200 L-210 L-220 Luxmeters. Instruction manual. Available online: https://www.sonopan.com.pl/en/download/2019/02/P-200-instruction-manual-2018-12-12.pdf (accessed on 7 March 2026).
35. Collin A.J.; Djokic, S.Z.; Drapela, J.; Langella, R.; Testa, A. Light flicker and power factor labels for comparing LED lamp performance. *IEEE Transactions on Industry Applications* **2019**, 55(6), pp. 7062-7070, doi: https://doi.org/10.1109/TIA.2019.2919643
36. Rashid, M.H. Power Electronics Handbook, 3rd ed., Elsevier: Amsterdam, The Netherlands, 2011.
37. Abdalaal, R.M.; Ho, C.N.M. Characterization of commercial LED lamps for power quality studies. In Proceedings of *2017 IEEE Electrical Power and Energy Conference (EPEC)*, Saskatoon, Saskatchewan, Canada, 22-25 October 2017.
38. Winder, S. Power Supplies for LED Driving, 2nd ed.; Elsevier BV: Aalborg, Denmark, 2017.
39. Beaty, W.H. Handbook of Electric Power Calculations, 3rd ed., McGraw-Hill: New York, NY, USA, 2012.
40. Górecki, K.; Posobkiewicz, K. Influence of the selection of the approximating function of thermometric characteristics on the measurement results of thermal resistance of power MOSFETs. *Metrol. Meas. Syst.* **2024**, 31, pp. 307–321, doi: https://doi.org/10.24425/mms.2024.149702

 doi:10.20944/preprints202603.1372.v1

41. Sikora, R.; Markiewicz, P. Analysis of electric power quantities of road LED luminaires under sinusoidal and non-sinusoidal conditions. *Energies* **2019**, 12(6), 1109, doi: https://doi.org/10.3390/en12061109
42. Peretto, L.; Tinarelli, R.; Rovati, L.; Bernabei, M. On the behavior of LED lamps under non-sinusoidal voltage conditions. In *2017 IEEE International Instrumentation and Measurement Technology Conference (I2MTC)*, Turin, Italy, 22-25 May 2017**.**
43. Rojas-Osorio, E.; Saavedra-Montes A.J.; Ramos-Paja C. A.; Effect of the Harmonic Voltage Distortion on the Efficiency of a Compact Fluorescent Lamp. *Revista Facultad de Ingeniería* **2020**, 29(54), doi: https://doi.org/10.19053/01211129.v29.n54.2020.11604